Taylor & Francis
Taylor & Francis Group

Journal of the Air & Waste Management Association

ISSN: 1096-2247 (Print) 2162-2906 (Online) Journal homepage: http://www.tandfonline.com/loi/uawm20

The effects of emission control strategies on light-absorbing carbon emissions from a modern heavy-duty diesel engine

Michael A. Robinson, Michael R. Olson, Z. Gerald Liu & James J. Schauer

To cite this article: Michael A. Robinson, Michael R. Olson, Z. Gerald Liu & James J. Schauer (2015) The effects of emission control strategies on light-absorbing carbon emissions from a modern heavy-duty diesel engine, Journal of the Air & Waste Management Association, 65:6, 759-766, DOI: 10.1080/10962247.2015.1005850

To link to this article: http://dx.doi.org/10.1080/10962247.2015.1005850

View supplementary material

Accepted author version posted online: 20 Jan 2015.
Published online: 20 Jan 2015.

Submit your article to this journal

Article views: 503

View related articles

View Crossmark data

Citing articles: 3 View citing articles

Full Terms & Conditions of access and use can be found at
http://www.tandfonline.com/action/journalInformation?journalCode=uawm20

Download by: [University of North Texas] **Date:** 26 December 2016, At: 02:14

TECHNICAL PAPER

The effects of emission control strategies on light-absorbing carbon emissions from a modern heavy-duty diesel engine

Michael A. Robinson,[1,*] Michael R. Olson,[2] Z. Gerald Liu,[1] and James J. Schauer[2]

[1]*Cummins Emission Solutions, Inc., Stoughton, WI, USA*

[2]*University of Wisconsin–Madison, Madison, WI, USA*

[*]*Please address correspondence to: Michael A. Robinson, Cummins Emission Solutions, Inc., Analysis and Testing Technologies, 1801 U.S. Hwy 51, Stoughton, WI 53589, USA; e-mail: ja665@cummins.com*

Control of atmospheric black carbon (BC) and brown carbon (BrC) has been proposed as an important pathway to climate change mitigation, but sources of BC and BrC are still not well understood. In order to better identify the role of modern heavy-duty diesel engines on the production of BC and BrC, emissions from a heavy-duty diesel engine operating with different emission control strategies were examined using a source dilution sampling system. The effect of a diesel oxidation catalyst (DOC) and diesel particulate filter (DPF) on light-absorbing carbon (LAC) was evaluated at three steady-state engine operation modes: idle, 50% speed and load, and 100% speed and load. LAC was measured with four different engine configurations: engine out, DOC out, DPF out, and engine out with an altered combustion calibration. BC and BrC emission rates were measured with the Aethalometer (AE-31). EC and BC emission rates normalized to the mass of CO_2 emitted increased with increasing engine speed and load. Emission rates normalized to brake-specific work did not exhibit similar trends with speed and load, but rather the highest emission rate was measured at idle. EC and OC emissions were reduced by 99% when the DOC and DPF architecture was applied. The application of a DPF was equally effective at removing 99% of the BC fraction of PM, proving to be an important control strategy for both LAC and PM. BC emissions were unexpectedly increased across the DOC, seemingly due to a change aerosol optical properties. Removal of exhaust gas recirculation (EGR) flow due to simulated EGR cooler failure caused a large increase in OC and BrC emission rates at idle, but had limited influence during high load operation. LAC emissions proved to be sensitive to the same control strategies effective at controlling the total mass of diesel PM.

Implications: In the context of black carbon emissions, very small emission rates of brown carbon were measured over a range of control technologies and engine operating conditions. During specific idle engine operation without EGR and adjusted fueling conditions, brown carbon can be formed in significant amounts, requiring careful management tactics. Control technologies for particulate matter are very effective for light-absorbing carbon, reducing black carbon emissions to near zero for modern engines equipped with a DPF. Efforts to control atmospheric brown carbon need to focus on other sources other than modern diesel engines, such as biomass burning.

Introduction

Black carbon (BC) is a solid form of carbon that strongly absorbs light independent of wavelength. Brown carbon (BrC) is a made up of organic carbon compounds that absorb light strongly in the near ultraviolet range. Light-absorbing carbon (LAC) may play significant roles in the direct radiative forcing of the atmosphere (Shindell et al., 2012; Feng et al., 2013). Light-absorbing carbon (LAC), mainly emitted from uncontrolled combustion sources, strongly absorbs solar radiation, converting electromagnetic energy to thermal energy, causing a localized increase in atmospheric temperatures (Bond and Bergstrom, 2006; Moosmüller et al., 2009). In 2005, diesel particulate matter (PM) was found to be one of the major three sources of black carbon (BC) particles in the United States (U.S. Environmental Protection Agency [EPA], 2012). Rigorous emission regulations for diesel engines have been implemented since 2005, mandating a reduction in PM by an order of magnitude. These regulations have been shown to be effective at reducing local ambient BC concentrations in California (Bahadur et al., 2011). The reduction of BC particles due to tight control on diesel combustion sources, however, does not imply total LAC reduction. This uncertainty in LAC emission rates necessitates accurate measurements of optical properties and thus the possible radiative forcing potential of diesel PM. These measurements are critical to understanding the possible environmental impacts of emission control strategies for diesel PM.

Modern diesel PM, before exhaust aftertreatment (AT), can be conceptualized as a solid core of elemental carbon (EC) particles covered with a coating of condensed organic carbon

Journal of the Air & Waste Management Association, 65(6):759–766, 2015. Copyright © 2015 A&WMA. ISSN: 1096-2247 print
DOI: 10.1080/10962247.2015.1005850 Submitted September 29, 2014; final version submitted December 19, 2014; accepted January 5, 2015.

(OC) and sulfates (Maricq, 2007). Various techniques are available to reduce PM and other criteria pollutant formation in-cylinder, including, but not limited to, fuel injection pressure, start of injection (SOI), and exhaust gas recirculation (EGR). High fuel pressure and advanced SOI generally promote fuel–air mixing and fuel atomization, reducing overall PM formation mechanisms but increasing thermal nitrogen oxides (NOx) formation (Kweon et al., 2003). The application of EGR is commonly used to reduce adiabatic flame temperature, thereby reducing NOx emissions at the penalty of increased PM emissions. This well-known NOx–PM trade-off of conventional diesel combustion (CDC) currently requires the application of advanced AT to meet U.S. and European emission standards for PM, NOx, carbon monoxide (CO), and unburned hydrocarbons (UHCs) (Zheng et al., 2004). The complex interaction of in-cylinder control and AT effect on PM is important in understanding and ultimately controlling LAC.

Diesel AT development, mainly in the on-highway market, has accelerated rapidly since the turn of the century due to the aforementioned regulatory requirements. The diesel oxidation catalyst (DOC), which has the primary role of catalytically reducing CO and UHCs in the gas phase, is also known to affect the volatile fraction of PM (Vaaraslahti et al., 2006). Diesel particulate filters (DPFs) have been developed to remove diesel PM at 99% by mass (Liu et al., 2003). High-efficiency NOx reduction AT such as selective catalytic reduction (SCR) has recently reached deNOx performance greater than 95% due to new catalyst formulations and control techniques (Johnson, 2012). Due to the most stringent emissions regulations in both the United States and Europe, the on-highway market of diesel power trains has the common architecture of DOC + DPF + SCR. The off-highway market of diesel engine-powered vehicles is facing increasing scrutiny from regulators, facing EPA Tier 4 Final emission regulations in 2014. Due to differences in duty cycle, power ratings, and a huge variety of applications, the off-highway sector faces a complex engineering problem when considering AT and in-cylinder control strategies. Some applications may employ a DOC + SCR AT architecture, without EGR, due to high SCR deNOx efficiency and in-cylinder PM reduction (Ohrnberger et al., 2012). The lack of a wall flow DPF for these off-highway applications further emphasizes the importance of understanding various control strategies' effect on LAC.

Due to the physical and chemical differences between LAC and criteria pollutants, it is unclear what effect AT and in-cylinder control will have on BC and BrC. New technology diesel exhaust (NTDE) has been shown to have a large portion of nucleation mode (<50 nm) organic carbon (OC) particles and sulfates as compared to traditional diesel exhaust (TDE), which is classically thought to be composed of mainly larger (>100 nm) elemental carbon particles (Hesterberg et al., 2011). These changes in NTDE PM chemical composition and particle size indicate possible changes in NTDE PM optical properties. Engine operation and AT effect on diesel PM chemical composition are well understood; however, how these factors affect aerosol optical properties is not well documented in literature (Kweon et al., 2003). These changes in PM chemical composition and AT architecture necessitate improved understanding of optical measurements to quantify BC and BrC to assess possible strategies to control LAC.

BC measurements are commonplace in the ambient monitoring domain; however, limited application of optical instrumentation to quantify BC or BrC emission rates to diesel engines is available for modern technologies. Ng et al. (2007) provide an excellent comparison of the Aethalometer (AE-16, Magee Scientific) to common diesel PM measurement techniques. However, the study utilized 350-ppm-sulfur fuel and did not investigate the influence of AT or EGR. The photoacoustic method, which has been well documented as a standard for BC measurement, has been applied to some engine source measurements (Moosmüller et al., 2009; Arnott et al., 2005). A photoacoustic instrument was not available for the entirety of this study but a comparison of BC measurement methods is provided by Robinson et al. (2014). A recent data set showed positive correlation between the AE-31, the photoacoustic method, and the thermo-optical method (Robinson et al., 2014). The objectives of this study are to characterize how operating condition and emission control strategy may affect the heavy-duty diesel engine emission rates of BC and BrC as compared to standard thermo-optical-transmittance methods.

Experimental Methods

Test equipment and procedures

Diesel PM was generated and sampled at the Cummins Emission Solutions constant volume sampling (CVS) lab in Stoughton, WI. The diesel engine under investigation was a heavy-duty on-highway engine (model ISX15 MY2010, displacement 14.9 L, rated power 373 kW at 1800 rpm, peak torque 2508 N-m at 1200 rpm, Cummins, Inc.) equipped with cooled high-pressure EGR, high-pressure common rail fuel injection system, and variable-geometry turbocharger. In addition to the in-cylinder control strategies, the full engine system is typically installed into class 8 long-haul trucks with an advanced AT system comprised of a cordierite flow-through DOC, coated cordierite wall flow DPF, and SCR system to meet EPA 2010 on highway emission standards. The aftertreatment system used during this study was aged for approximately 200 hr on engine before use and was preconditioned for 30 min at the A25 engine mode before samples were taken. The SCR system was not used during this work, as the SCR effect on PM mass, EC, and OC is mimimal, and its expected effect on BC and BrC will be similar (Liu et al., 2008; Biswas et al., 2009). During the course of sampling, the CVS test cell was reconfigured with different engine control module (ECM) calibrations and AT configurations to elucidate the effect on the emitted aerosols optical properties.

EGR was turned off during portions of the sampling campaign to emulate an engine calibration developed for low NOx without EGR. The manner in which the EGR system was disabled was meant to simulate an on-board diagnostic detected failure in the EGR cooler. When such a failure is detected, the EGR valve closes completely and fuel injection parameters are changed to reduce NOx formation in cylinder. Main SOI and fuel rail pressure are two major control parameters available when EGR flow is removed. In this ECM calibration, to reduce

Table 1. Engine operation modes

	Idle	B50	C100
Speed	650 rpm	1555 rpm	1912 rpm
Load	10%	50%	100%
EGT	128°C	341°C	424°C

thermal NOx formation, main SOI is retarded to prevent intense premixed combustion during the compresssion process. Unless a designation of "EGR Off" is noted, the commerical ECM calibration for this engine was used during the rest of the study.

The engine was operated over three hot steady-state operating points using a dynamometer (Direct Current, GE Co). Operating modes were chosen from the EPA ramped modal cycle suplemental emission test (RMCSET), which spanned the full operating map. Engine operation mode details such as speed, load, and exhaust gas temperature (EGT) can be found in Table 1. Diesel fuel used in this study had a cetane number of 47.4 with a specific gravity of 845.0 kg/m^3 and a sulfur content of 6 ppm. Further fuel specifications can be found in Supplemental Table 1. Full engine exhaust was piped into a critcal flow Venturi (CFV) CVS tunnel, where the exhaust was mixed with activated carbon and HEPA-filtered air. Primary dilution ratio between the dilution air and the exhaust gas varied between 2:1 and 13:1 depending on the engine operating mode and AT configuration. A partial flow sample was secondarily diluted in the source dilution sampling (SDS) system, 10 tunnel diameters downstream of the primary dilution mixing plane (Liu et al., 2008). Primary and secondary dilution air were maintained at room temperature (20 ± 2°C). Secondary dilution ratio was varied from 2:1 to 30:1 depending on engine operation and AT configuration in order to optimize filter-based analytics. The effects of dilution conditions on particle condensation and nucleation during the dilution process have been studied by many researchers and were taken into careful account when designing the secondary microdiluter (Liu et al., 2008). The full test cell schematic can be found in Figure 1. In order to decouple the fuel consumption dependence of engine emission rates, all rates are normalized to the mass of CO_2 emitted during the sampling period. Concentrations of other carbon-containing compounds (i.e., carbon monoxide, volatile OC) were not included in the normalization due to the low concentrations, relative to CO_2, in typical diesel exhaust (Yanowitz et al., 2000). For other species (EC, OC, and BrC), emission rates are calculated in the same manner.

Measurement methods

Dilute exhaust gas was sampled from the residence time chamber (RTC) after secondary dilution in the SDS. Quartz fiber filters (QFF) were sampled and analyzed via the NIOSH 5040 method for elemental carbon and organic carbon (EC and OC, respectively) concentrations. An Aethalometer (AE-31, Magee Scientific) was used to measure multiple-wavelength attenuation. All AE-31 wavelengths were corrected for the reduction of the optical path, that is, filter loading via a multiple linear regression method. Test and wavelength specific loading correction factors were determined as a function of total attenuation reported by the AE-31 from the time of filter tape advance. BC mass concentrations were determined at 880 nm with a constant EC specific attenuation cross section (σ_{atn}) of 25.4 ± 1.30 m^2 g^{-1}. Calculation of σ_{atn} is shown in Figure 2, where dashed lines represent 95% confidence intervals on the

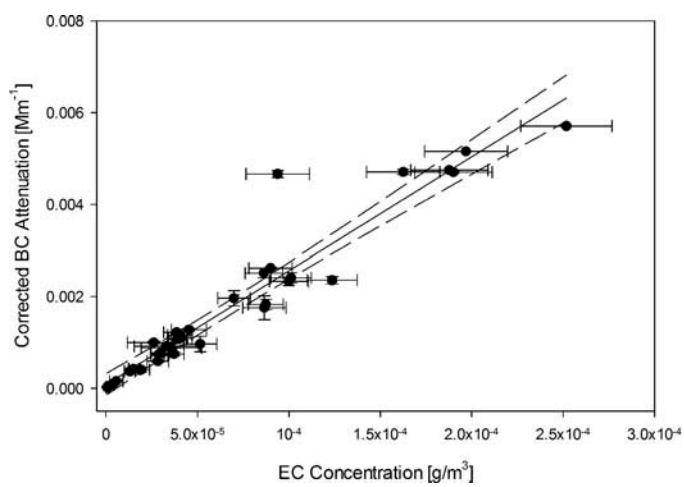

Figure 2. Determination of σ_{atn} at 880 nm.

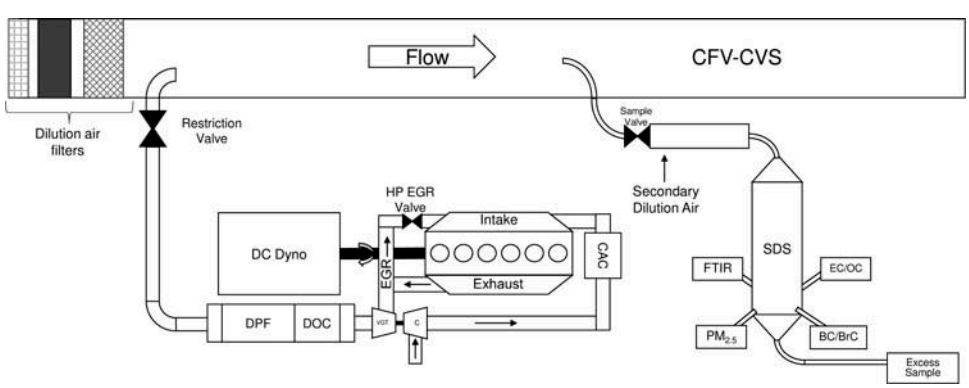

Figure 1. Test cell layout.

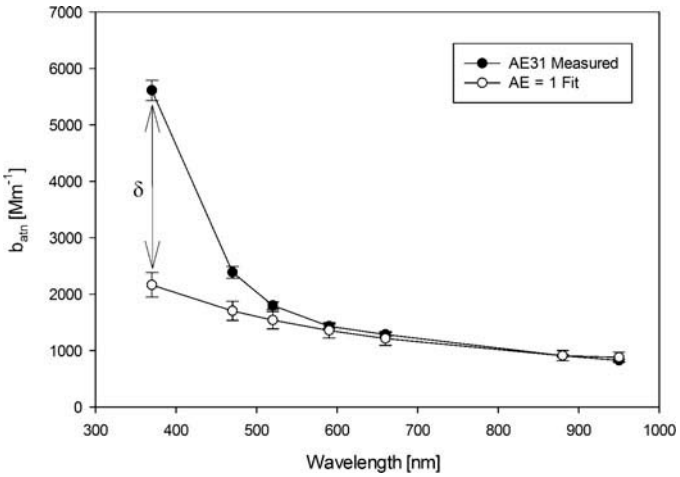

Figure 3. An example of BrC determination method (idle EGR off).

slope (R^2 = 0.918). The direct application of a test specific σ_{atn} accounts for multiple scattering in the filter media.

BrC determination was done using an Ångström exponent methodology described by Lack and Langridge and others (Lack, 2013; Andreae, 2006; Kirchstetter, 2004), an example of which can be found in Figure 3. An absorption Ångström exponent (AE) = 1 was fit to the experimentally measured attenuation coefficient at 880 nm, as shown in eq 1:

$$\mathrm{AE}(\lambda_1\lambda_2) = \frac{\log\left(\frac{b_{atn}(\lambda_1)}{b_{atn}(\lambda_2)}\right)}{\log\left(\frac{\lambda_1}{\lambda_2}\right)} \quad (1)$$

The difference (δ) in the measured attenuation coefficients and the AE = 1 attenuation coefficients is attributed to the BrC light absorption. BrC was reported at the 370-nm channel with a mass specific cross section of 60.4 $m^2\ g^{-1}$. The relationship between BrC absorption and mass specific cross section is shown in eq 2. The mass specific cross section for 370 nm was determined using eq 1 and the predetermined σ_{atn} of 25.4 $m^2\ g^{-1}$ at 880 nm. Only cases where both BrC attenuation was larger than measurement uncertainty and AE = 1 fit uncertainty were reported:

$$m_{BrC} = \frac{\delta}{\sigma_{atn,370}} \quad (2)$$

The reason for using this wavelength is twofold: First, it is commonly used in atmospheric monitoring literature to define BrC (Cheng et al., 2011; Hecobian et al., 2010; Thompson et al., 2012). Second, this wavelength is the limit of solar radiation that reaches the troposphere; all lower wavelengths are filtered by gases in the upper reaches of the troposphere.

Each AT configuration (engine out, DOC out, and DPF out) was investigated to understand the component level effect of AT on LAC emissions. Emission control strategies were evaluated for species-specific reduction efficiencies at each engine operation mode; this calculation is shown in eq 3:

$$\eta_i = -\frac{(ER_{i,IN} - ER_{i,OUT})}{ER_{i,IN}} * 100\% \quad (3)$$

where ER is the CO_2 specific emission rate for species i (EC, OC, and BC). The inlet condition for each emission control strategy was engine out with EGR. The species specific reduction efficiencies, η, are tabulated in Table 2.

Three data points for each engine operation mode and emission control strategy (AT or EGR) were taken, except for the DPF out condition due to the extremely long sample time required to reach the detection limits of the optical instrumentation. Error bars in the following figures represent either standard error of the three samples or the propagated analytical uncertainty.

Results and Discussion

The application of a DOC and DPF effectively reduced EC emission rates by 98% or greater, independent of engine operation mode. EC emission rates as a function of engine operation mode and AT configuration are shown in Figure 4. Brake-specific EC emission rates as a function of engine operation mode and AT configuration are shown in Supplemental Figure 1. The nonvolatile graphene nature of EC particles implies low expected reduction efficiencies across the DOC, as it was not developed to reduce the solid particle fraction (Vaaraslahti et al., 2006;

Table 2. Species specific reduction efficiencies for tested emission control strategies with associated uncertainties

Engine operation	Species	EGR effect	±	DOC effect	±	DOC + DPFeffect	±
Idle	EC	2%	22%	22%	13%	–99.1%	0.4%
	OC	436%	38%	–74%	4%	–94.0%	0.4%
	BC	–7%	2%	20%	3%	–99.2%	0.04%
B50	EC	30%	10%	34%	11%	–98.3%	0.2%
	OC	–2%	9%	–50%	7%	–93.5%	0.5%
	BC	0%	3%	74%	10%	–99.2%	0.06%
C100	EC	–85%	2%	–16%	7%	–99.9%	0.04%
	OC	–46%	6%	–74%	5%	–97.8%	0.2%
	BC	–80%	2%	8%	8%	–99.7%	0.03%

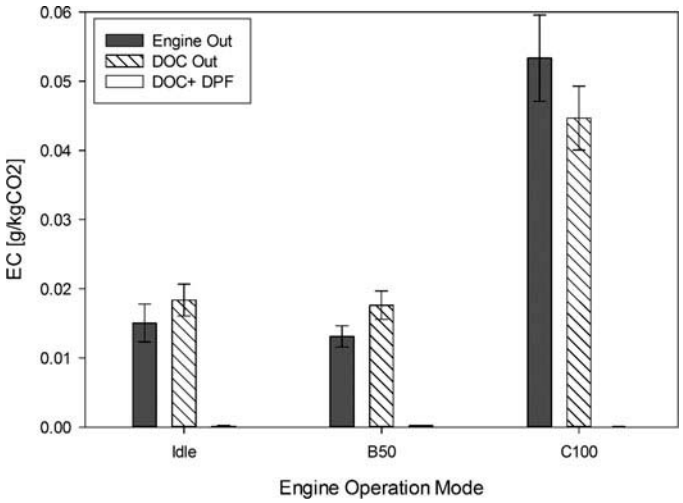

Figure 4. Effect of AT on EC emissions rates as a function of engine operation.

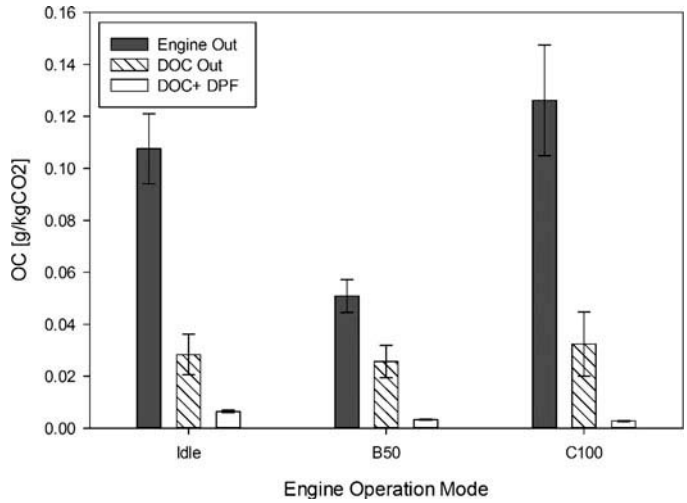

Figure 5. Effect of AT on OC emission rates as a function of engine operation.

Farrauto and Voss, 1996; Maricq et al., 2002). The results in Figure 4 show no detectible reduction in EC emissions under the DOC test condition. Due to low EGTs at the idle engine condition, the DOC has not reached light-off temperature. The B50 engine condition produces significantly higher EGT due to the increase in load and speed as compared to the idle condition. This increase in temperature may promote catalyzed oxidation of the engine out OC fraction across the DOC, explaining the 34 ± 11% increase of EC at the B50 engine mode. The oxidative cracking, oxidation, and dehydrogenation of compounds that make up the OC fraction have been well documented in bench-top reactor studies and may account for the observed increase (Collura et al., 2005; Atribak et al., 2010; Silberova et al., 2003). However, the error bars shown in Figure 4 indicate the measured increase in EC is uncertain. Finally, the C100 engine operation mode, which has the highest EGT, displayed the highest EC reduction of 16 ± 7% when exhaust gas is treated with the DOC. The DPF was highly effective at EC control across all three engine modes; similarly impressive results were observed for the OC fraction, which are discussed in the following.

Total OC fraction emission rates are reduced by 93% or greater when the DOC and DPF are applied. OC emission rates as a function of engine operation mode are shown in Figure 5. Brake-specific OC emission rates as a function of engine operation mode and AT configuration are shown in Supplemental Figure 2. The DOC is much more efficient at removing the OC fraction as compared to the EC fraction due to the increased volatility of the OC compounds and the gas-phase functionality of the DOC (Farrauto and Voss, 1996). The idle engine mode displayed the highest OC reduction of 74 ± 4% across the DOC, due to the easily oxidized low-volatile compounds emitted at idle. The C100 engine mode exhibited an equally high OC removal efficiency of 74 ± 5% across the DOC due to the high EGT, ensuring optimal operating conditions. The B50 engine mode demonstrated the lowest OC removal efficiency of 50 ± 7%. The combination of the DOC and DPF system reduced the OC fraction by 94.0 ± 0.4 %, 93.5 ± 0.5 %, and 97.8 ± 0.2 % for idle, B50, and C100, respectively. As reported in Hesterberg et al. (2011), a portion of the engine out OC fraction is not removed with the DPF, albeit small.

The DOC and DPF display equally impressive reduction efficiency for the BC fraction of the PM, reducing the BC by more than 99%. BC emission rates as a function of engine operation mode and AT configuration are shown in Figure 6. Brake-specific BC emission rates as a function of engine operation mode and AT configuration are shown in Supplemental Figure 3. Engine-out BC emission rates are very similar to EC emission rates (shown in Figure 4), as EC is the strongest light-absorbing component of diesel PM. However, after the DOC treated the exhaust, an increase in BC emission rates was observed for two of the three engine modes. An increase in BC emissions of 20 ± 3% was measured at idle, 74 ± 10% at B50, and 8 ± 8% at C100. Conventional wisdom would predict a decrease in BC emissions across the DOC due to a reduction in OC emissions and the associated lensing effect (Bond et al., 2006). However, this lensing effect

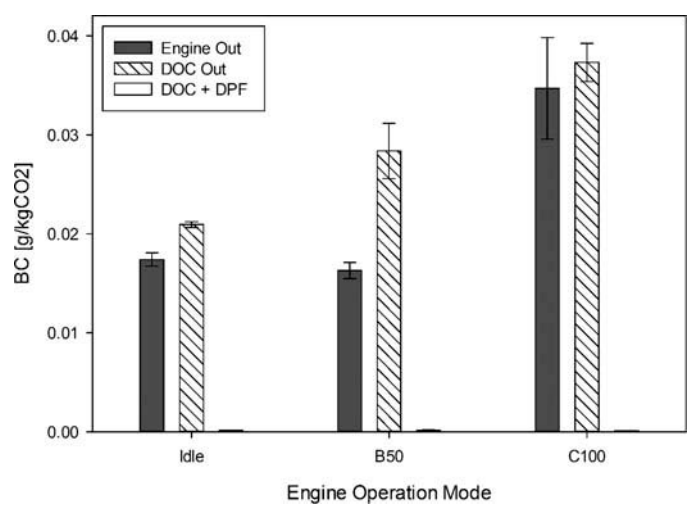

Figure 6. Effect of AT on BC emission rates as a function of engine operation.

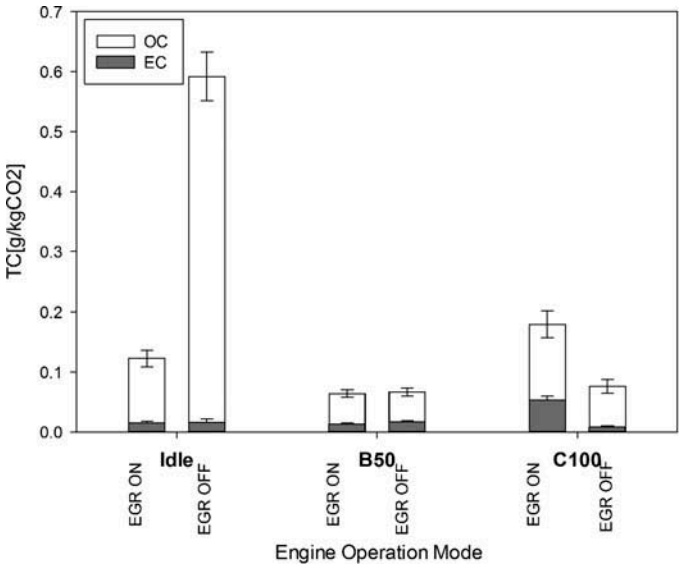

Figure 7. Effect of EGR on EC/OC emission rates.

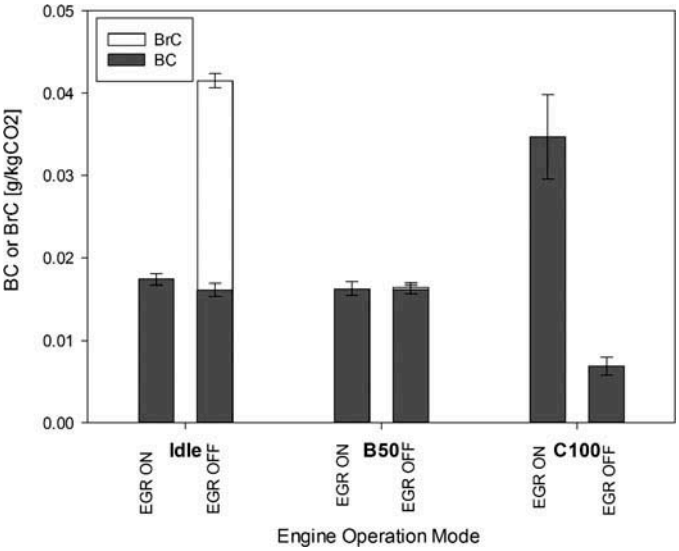

Figure 8. Effect of EGR on BC and BrC emission rates.

was not observed for freshly emitted aerosols. The increase in BC emission rates due to DOC treatment is an indication that the chemical and physical properties of the aerosol have changed enough to affect the optical properties as measured by the Aethalometer. The DOC and DPF proved to be efficient at reducing BC emissions. Reduction efficiencies of BC we measured at greater than 99.2% across the DOC and DPF system. Thus, even with an increase in BC emissions across the DOC, application of a wall flow DPF has been shown to reduce BC emission rates to ultra-low levels. However, certain off-highway and emerging market applications are able to meet $PM_{2.5}$ regulations without use of a DPF, relying solely on in-cylinder techniques and DOC PM reduction.

CDC relies heavily on EGR mass fraction in certain areas of the engine map where SCR efficiency is temperature limited, but with this NOx reduction comes an increase in PM formation (Zheng et al., 2004). Combustion recipe changes associated with turning EGR off at the idle condition have limited effect on the EC fraction of the PM emitted. A more substantial increase in EC emissions associated with the EGR-off ECM calibration was measured at the B50 engine condition, with EC emission rate increasing by 30 ± 10%. The most significant change to EC emission rates due to the EGR-off ECM calibration was measured at the C100 engine condition, decreasing EC emission rates by 85 ± 2%. The effect of the "EGR-off" ECM calibration on engine-out EC and OC emission rates is shown in Figure 7. Brake-specific EC and OC emission rates as a function of engine operation mode and combustion calibration are shown in Supplemental Figure 4. Changes to the combustion strategy have a much more significant effect on the OC emission rates at the idle engine condition, increasing OC emission rates by 436 ± 36%. The B50 engine condition saw little change in OC emission rates due to the "EGR-off" strategy. Reduction trends continued at the C100 engine condition, as changes yielded a 46 ± 6% reduction in OC emission rates. Reduction of EGR mass fraction is classically thought to reduce overall PM mass emissions in CDC due to an increase in PM oxidation rates in cylinder due to increased temperatures and O_2 concentrations. This phenomenon holds true for the C100 engine condition, which displayed the most significant decreases in both the EC and OC fractions. However, at low load conditions, such as idle, EGR flow can raise charge temperatures by 30°C, increasing the final compressed mixture temperature before fuel injection. This increase in final mixture temperature improves soot oxidation rates in cylinder, reducing the volatile OC fraction. In addition to this increased temperature, retarded main injection timing to prevent NOx formation decreases mixing times, likely increasing local equivalence ratios.

BC emission rates displayed similar trends to EC emission rates when EGR was turned off; this aligns well with trends revealed as a function of AT. Both high speed and load points displayed BC dominating the LAC emissions with both combustion strategies. Idle showed a dramatic increase in measured BrC emissions when EGR was turned off. This increase from a non–detect to 0.025 [g/kgCO_2], makes up almost 61% of the LAC emissions during the idle engine mode. The effects of EGR on engine out BC and BrC emission rates are shown in Figure 8. Brake specific BC and BrC emissions rates as a function of engine operation mode and combustion calibration are shown in Supplemental Figure 5. The measured BrC emissions at idle without EGR are likely due to the large fraction of OC emitted. OC chemical composition was not determined during this work, but would likely resolve differences in BrC emissions from differing combustion calibrations and engine operation modes. BrC particles absorb light less efficiently than BC due to its chemical makeup and its associated refractive index, requiring much higher concentrations to contribute to overall light absorption by the aerosol.

Conclusions

Test cell dynamometer measurements of BC and BrC as a function of engine operation and emission control strategy

exposed numerous trends in LAC emissions. The application of the DPF has displayed exceptional control for diesel combustion generated BC during steady-state operation across the operating map. Engine out emission rates of BC correlate well with EC emission rates across the operation map, which is consistent with similar studies (Ng et al., 2007; Arnott et al., 2005). The DOC is effective at reducing a portion of the OC fraction, which in turn affects the optical properties of the aerosol, increasing BC emission rates post DOC. This effect is not significant enough to lessen the importance of the DOC on criteria pollutants control. An ambient absorption Ångström exponent method was used to quantify BrC particles, at the 370-nm wavelength. During the course of this work, BrC aerosols were not common, due to the relatively low concentrations of OC emitted during normal engine operation. However, similar to recently published work, during specific engine operation, diesel PM can exhibit absorption Ångström exponents greater than 1 (Guo et al., 2014). In this case, changes in the combustion calibration meant to mimic EGR cooler failure, including the removal of EGR flow and retardation of main SOI, caused a significant OC particle emission rate increase at the idle engine mode. The absorption of light by these OC particles, deemed BrC, increased overall LAC emission rates by 61% at the idle engine mode. Transient cold- and hot-start LAC emission rates still need evaluation, as it is unclear from this work whether similar reduction trends will see during transient test cycles. This work will require more capable instrumentation, as the version of the Aethalometer used in this work is limited to steady-state testing. The initial results of quantifying LAC emissions from diesel combustion show effective application of ambient LAC methods. Modern diesel PM control methods proved to be effective in reducing BC to near-zero emission rates.

Acknowledgments

The authors acknowledge Paul Van Rooy and Austin Yantes of University of Wisconsin–Madison, Environmental Chemistry and Technology Department, for help with setup and test execution. The authors also acknowledge Niklas Schmidt, Chris Cremeens, Nick Molzahn, Dustin Esteltine, Brad Nolley, and Jason Cassidy of Cummins Emission Solutions for their assistance with parts procurement, sampling, and testing support, as well as Shawn Hricko of Cummins Engine Business Unit for engine calibration support.

Funding

This publication was made possible in part by EPA grant 83503901. Its contents are solely the responsibility of the grantee and do not necessarily represent the official views of the EPA. Further, the EPA does not endorse the purchase of any commercial products or services mentioned in the publication.

Supplemental Materials

Supplemental materials for this article can be accessed at http://dx.doi.org/10.1080/10962247.2015.1005850

References

Andreae, M.O., and A. Gelencser. 2006. Black carbon or brown carbon? The nature of light-absorbing carbonaceous aerosols. *Atmos. Chem. Phys*. 6:3131–3148. www.atmos-chem-phys.net/6/3131/2006. doi:10.5194/acp-6-3131-2006

Arnott, W.P. B. Zielinska, C.F. Rogers, J. Sagebiel, K. Park, J. Chow, H. Moosmüller, J.G. Watson, K. Kelly, D. Wagner, A. Sarofim, J. Lighty, and G. Palmer. 2005. Evaluation of 1047-nm photoacoustic instruments and photoelectric aerosol sensors in source-sampling of black carbon aerosol and particle-bound PAHs from gasoline and diesel powered vehicles. *Environ. Sci. Technol*. 39:5398–5406. doi:10.1021/es049595e

Atribak, I., A. Bueno-Lopez, and A. Garcia-Garcia. 2010. Uncatalysed and catalysed soot combustion under NOx+O_2: Real diesel versus model soots. *Combust. Flame* 157:2086–2094. doi:10.1016/j.combustflame.2010.04.018

Bahadur, R., Y. Feng, L.M. Russell, and V. Ramanathan. 2011. Impact of California's air pollution laws on black carbon and their implications for direct radiative forcing. *Atmos. Environ*. 45:1162–1167. doi:10.1016/j.atmosenv.2010.10.054

Biswas, S., V. Verma, J.J. Schauer, and C. Sioutas. 2009. Chemical speciation of PM emissions from heavy-duty diesel vehicles equipped with diesel particulate filter (DPF) and selective catalytic reduction (SCR) retrofits. *Atmos. Environ*. 43(11):1917–1925. doi:10.1016/j.atmosenv.2008.12.040

Bond, T.C., and R.W. Bergstrom. 2006. Light absorption by carbonaceous particles: An investigative review. *Aerosol Sci. Technol*. 40(1):27–67. doi:10.1080/02786820500421521

Bond, T.C., G. Habib, and R.W. Bergstrom. 2006. Limitations in the enhancement of visible light absorption due to mixing state. *J. Geophys. Res*. 111(D20211). doi:10.1029/2006JD007315

Chakrabarty, R.K., H. Moosmuller, L.-W.A. Chen, K. Lewis, W.P. Arnott, C. Mazzoleni, M.K. Dubey, C.E. Wold, W.M. Hao, and S.M. Kreidenweis. 2010. Brown carbon in tar balls from smoldering biomass combustion. *Atmos. Chem. Phys*. 10:6363–6370. doi:10.5194/acp-10-6363-2010

Cheng, Y., K.-B. He, M. Zheng, F.-K. Duan, Z.-Y. Du, Y.-L. Ma, J.-H. Tan, F.-M. Yang, J.-M. Liu, X.-L. Zhang, R.J. Weber, M.H. Bergin, and A.G. Russell. 2011. Mass absorption efficiency of elemental carbon and water-soluble organic carbon in Beijing, China. *Atmos. Chem. Phys*. 11:11497–11510. doi:10.5194/acp-11-11497-2011

Collura, S., N. Chaoui, B. Azambre, G. Finqueneisel, O. Heintz, A. Krzton, A. Koch, and J.V. Weber. 2005. Influence of the soluble organic fraction on the thermal behaviour, texture and surface chemistry of diesel exhaust soot. *Carbon* 43:605–613. doi:10.1016/j.carbon.2004.10.026

Farrauto, R.J., and K.E. Voss. 1996. Monolithic diesel oxidation catalysts. *Appl. Catal. B Environ*. 10:29–51. doi:10.1016/0926-3373(96)00022-7

Feng, Y., V. Ramanathan, and V.R. Kotamarthi. 2013. Brown carbon: a significant atmospheric absorber of solar radiation? *Atmos. Chem. Phys*. 13:8607–8621. doi:10.5194/acp-13-8607-2013

Guo, X., T. Nakayama, H. Yamada, S. Inomata, K. Tonokura, and Y. Matsumi. 2014. Measurement of the light absorbing properties of diesel exhaust particles using a three-wavelength photoacoustic spectrometer. *Atmos. Environ*. 94:428–437. doi:10.1016/j.atmosenv.2014.05.042

Hansen, A.D.A. 2005. *The Aethalometer. Manual*. Berkeley, CA: Magee Scientific Company. http://www.mageesci.com/images/stories/docs/Aethalometer_book_2005.07.03.pdf.

Hecobian, A., X. Zhang, M. Zheng, N. Frank, E.S. Edgerton, and R.J. Weber. 2010. Water-soluble organic aerosol material and the light-absorption characteristics of aqueous extracts measured over the southeastern United States. *Atmos. Chem. Phys*. 10:5965–5977. doi:10.5194/acp-10-5965-2010

Hesterberg, T.W., C.M. Long, S.N. Sax, C.A. Lapin, R.O. McClellan, W.B. Bunn, and P.A. Valberg. 2011. Particulate matter in new technology diesel

exhaust (NTDE) is quantitatively and qualitatively very different from that found in traditional diesel exhaust (TDE). *J. Air Waste Manage. Assoc*. 61(9):894–913. doi:10.1080/10473289.2011.599277

Johnson, T. 2012. Vehicular emissions in review. *SAE Int. J. Engines* 5(2). doi:10.4271/2012-01-0368

Kirchstetter, T.W., T. Novakov, and P.V. Hobbs. 2004. Evidence that the spectral dependence on light absorption by aerosols is affected by organic carbon. *J. Geophys. Res. Atmos*. 109(D21208). doi:10.1029/2004JD004999

Kweon, C., S. Okada, J.C. Stetter, C.G. Christenson, M.M. Shafer, J.J. Schauer, and D.E. Foster. 2003. Effect of injection timing on detailed chemical composition and particulate size distributions of diesel exhaust. *SAE Tech. Paper 2003-01-1794*.

Lack, D.A., and J.M. Langridge. 2013. On the attribution of black and brown carbon light absorption using the Angstrom exponent. *Atmos. Chem. Phys*. 13(20):10535–10543. doi:10.5194/acp-13-10535-2013

Liu, G.Z., T.A. Swor, J.J. Schauer, J.J. Debilzen, et al. 2008. A source dilution sampling system for characterization of engine emissions under transient or steady-state operation. *Aerosol Sci. Technol*. 42(4):270–280. doi:10.1080/02786820801992907

Liu, Z.G., D.R. Berg, T.A. Swor, and J. J. Schauer. 2008. Comparative analysis on the effects of diesel particulate filter and selective catalytic reduction systems on a wide spectrum of chemical species emissions. *Environ. Sci. Technol*. 42(16):6080–6085. doi:10.1021/es8004046

Liu, Z.G., M.D. Skemp, and J.C. Lincoln. 2003. Diesel particulate filters: Trends and Implications of particle size distribution measurement. *SAE Tech. Paper 2003-01-0046*.

Maricq, M.M. 2007. Chemical characterization of particulate emissions from diesel engines: A review. *J. Aerosol Sci*. 38:1079–1118.

Maricq, M.M., R.E. Chase, N. Xu, and P.M. Laing. 2002. The effects of the catalytic converter and fuel sulfur level on motor vehicle particulate matter emissions: Light duty diesel vehicles. *Environ. Sci. Technol*. 36(2):283–289. doi:10.1021/es010962l

Moosmuller, H., R.K. Chakrabarty, and W.P. Arnott. 2009. Aerosol light absorption and its measurement: A review. *J. Quant. Spectrosc. Radiative Transfer* 110(11):844–878. doi:10.1016/j.jqrst.2009.02.035

Ng, I.P., H. Ma, D. Kittleson, and A. Miller. 2007. Comparing measurements of carbon in diesel exhuast aerosols using the Aethalometer, NIOSH Method 5040, and SMPS. *SAE Tech. Paper 2007-01-0334*. doi:10.4271/2007-01-0334

Ohrnberger, T., C. Becker, and C. Doehring. 2012. Assessment of Tier 4 Final aftertreatment strategies. *SAE Tech. Paper 2012-01-1953*. doi:10.4271/2012-01-1953

Robert, M.A., M.J. Kleeman, and C.A. Jakober. 2007. Size and composition distributions of particulate matter emissions: Part 2—Heavy-duty diesel vehicles. *J. Air Waste Manage. Assoc*. 57(12):1429–1438. doi:10.3155/1047-3289.57.12.1429

Robinson, M., Z.G. Liu, M. Olson, and J. Schauer. 2014. Comparison of measurement strategies for light absorbing aerosols from modern diesel engines. *SAE Int. J. Fuels Lubricants* 7:543–550. doi:10.4271/2014-01-1570

Shindell, D., J.C.I. Kulenstierna, E. Vignati, R. Dingenen, et al. 2012. Simultaneously mitigating near-term climate change and improving human health and food security. *Science* 335(13):183–189. doi:10.1126/science.1210026

Silberova, B., R. Burch, A. Goguet, C. Hardacre, and A. Holmen. 2003. Low-temperature oxidation reactions of ethane over a Pt/Al_2O_3 catalyst. *J. Catal*. 219:206–213. doi:10.1016/S0021-9517(03)00150-7

Thompson, J.E., P.L. Hayes, J.L. Jimenez, K. Adachi, X. Zhang, J. Liu, R.J. Weber, and P.R. Buseck. 2012. Aerosol optical properties at Pasadena, CA during CalNex 2010. *Atmos. Environ*. 55:190–200. doi:10.1016/j.atmosenv.2012.03.011

U.S. Environmental Protection Agency. 2012. Report to Congress on black carbon. http://www.epa.gov/blackcarbon/

Vaaraslahti, K., J. Ristimaki, A. Virtanen, J. Keskinen, B. Giechaskiel, and A. Solla. 2006. Effect of oxidation catalysts on diesel soot particles. *Environ. Sci. Technol*. 40(15):4776–4781. doi:10.1021/es060615h

Yanowitz, J., R.L. McCormick, and M.S. Graboski. 2000. In-use emissions from heavy-duty diesel vehicles. *Environ. Sci. Technol*. 34(5):729–740. doi:10.1021/es990903w

Zheng, M., G.T. Reader, and J.G. Hawley. 2004. Diesel engine exhaust gas recirculation—A review on advanced and novel concepts. *Energy Conversion and Management* 45:883–900. doi:10.1016/S0196-8904(03)00194-8

About the Authors

Michael A. Robinson is a research and development (R&D) engineer and **Z. Gerald Liu** is the director of R&D at Cummins Emission Solutions, in Stoughton, WI.

Michael R. Olson is a Ph.D. student in the Environmental Chemistry and Technology Program at University of Wisconsin–Madison, in Madison, WI.

James J. Schauer is a professor in the College of Engineering at the University of Wisconsin–Madison, in Madison, WI.